Source regions and transmission rates of whistlers

David KORONCZAY [1,2], Janos LICHTENBERGER [1,2], Mark CLILVERD[3], Craig RODGER[4], Fabien DARROUZET[5], Sylvain RANVIER[5], Stefan LOTZ[6], Tero RAITA[7], Nina CHERNEVA[8], Dmitry SANNIKOV[8], Robert MOORE[9]

Corresponding Author: david.koronczay@ttk.elte.hu Affiliations: (1) Department of Geophysics and Space Sciences, Eötvös University, Budapest, Hungary (2) Geodetic and Geophysical Institute, HAS, Sopron, Hungary (3) British Antarctic Survey, Cambridge, UK. (4) Department of Physics, University of Otago, Dunedin, New Zealand (5) Royal Belgian Observatory, Brussels, Belgium (6) Space Science Directorate, South African National Space Agency, Hermanus, South Africa (7) Sodankylä Geophysical Observatory, University of Oulu, Oulu, Finland (8) Institute of Cosmophysical Research and Radio Wave Propagation, Paratunka, Russia (9) Department of Electrical and Computer Engineering, University of Florida, FL, USA

Abstract AWDANet is a global network for monitoring the plasmasphere. It consists of 15 ground stations automatically detecting and analysing lightning generated VLF whistlers in real-time. In this study we determined the lightning source region corresponding to each whistler detector location. Our results remove earlier uncertainties and conform to theoretical expectations.

1. Context

• Whistlers are VLF (3-30 kHz) impulses generated by lightning, travelling along magnetic field lines, observable on the ground and/or in space • Through dispersive propagation in the plasma content of the magnetosphere, they acquire a frequency-time signal with a characteristic shape • Whistler measurements tell us about the plasma density in the plasmasphere • AWDANET is a global network providing real-time whistler detection and analysis (Lichtenberger 2010)

Open question: exact propagation path and source location of the detected whistlers

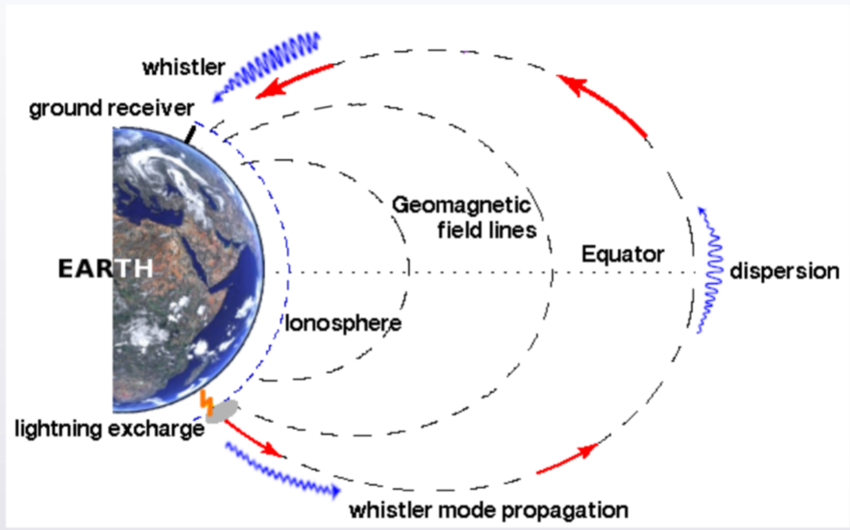

Fig. 1. Magnetospheric path of a single-hop ground-detected whistler from the source lightning to the receiver.

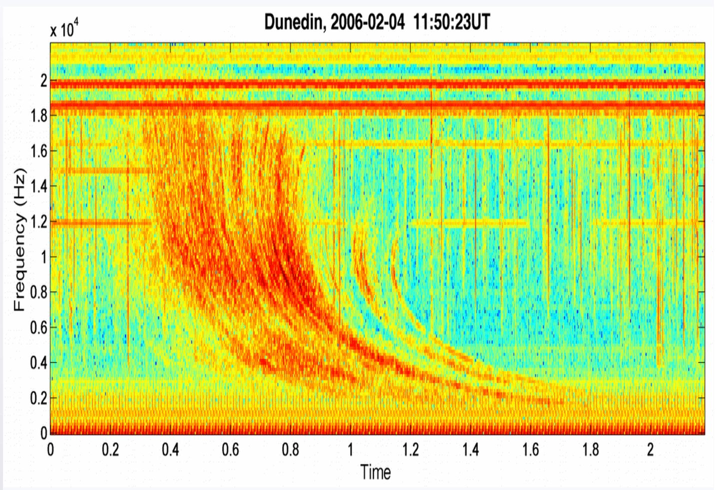

Fig. 2. Time-frequency spectrogram of a typical whistler group

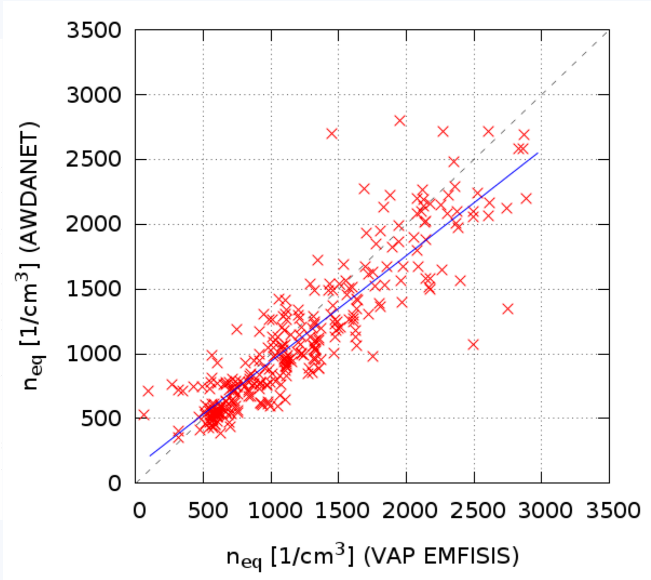

Fig. 3. Satellite based calibration of AWDANET-based plasmaspheric equatorial electron densities. (Lichtenberger 2017)

2. Data

Whistler data: AWDANET has been providing real-time data since 2014. In addition, for this study, we reprocessed archive raw data going back to 2007.

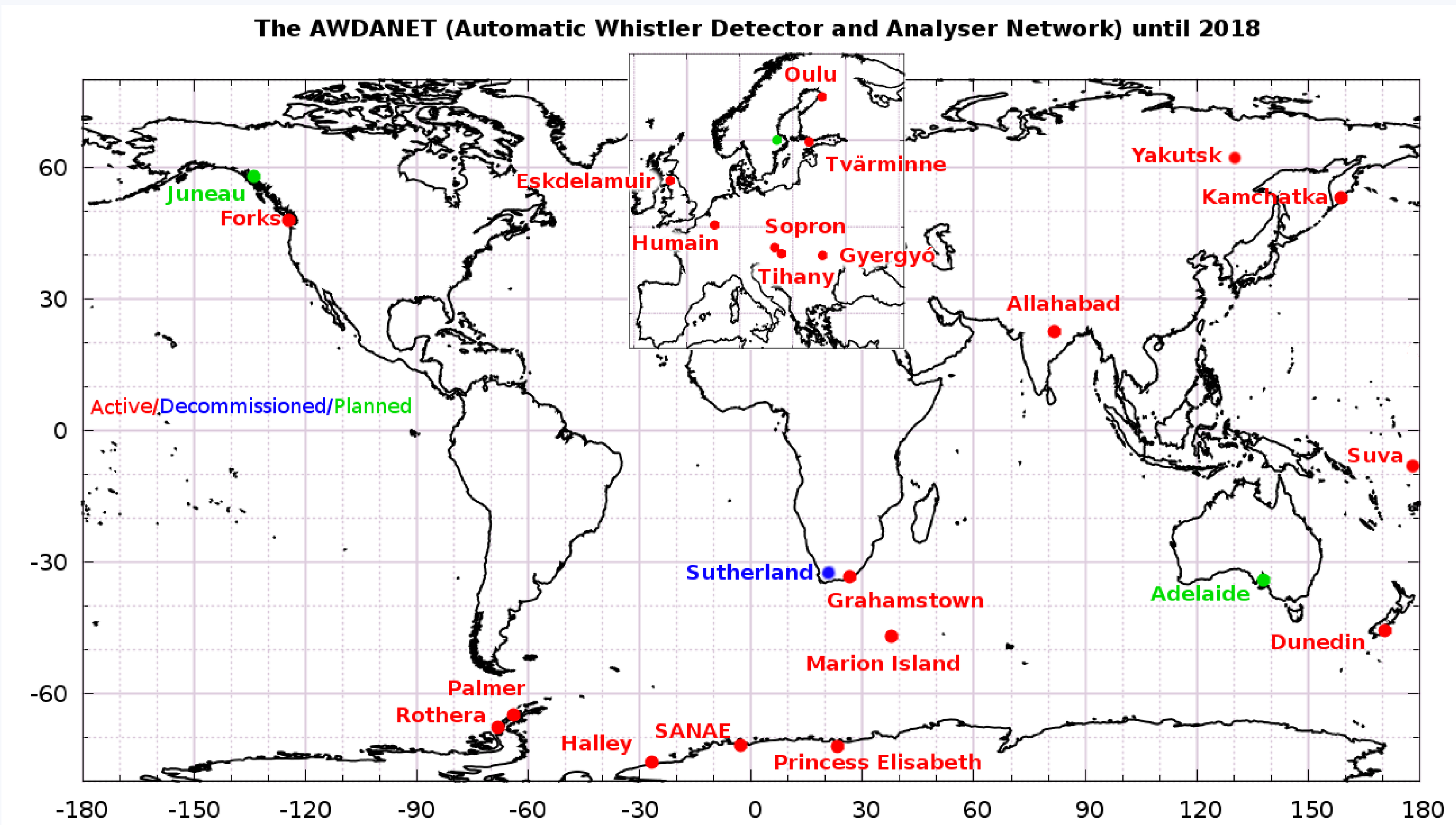

→ **Fig. 4.** Global map of AWDANET whistler detector stations, as of 2018.

Lightning data: the World Wide Lightning Location network (WWLLN) has been in operation since 2004, relying on its own VLF detector network and spheric analysis software. We accessed localized stroke dataset through collaboration. Or analysis involved 2 billion lightning strokes and ~70 million whistler events (see table).

Table 1. Whistler recordings processed in this study, in regional grouping

Station	Geodetic coordinates	L-value^a	Years processed	Total number of whistlers	Max. transmission ratio [%]
Dunedin	45.7°S, 170.5°E	2.78	2007-2017	3,660,000	75
Karymshina	53.0°N, 158.7°E	2.18	2012-2016	3,110,000	25
Palmer	64.8°S, 64.0°W	2.52	2009-2010	17,600,000	50
Rothera	67.5°S, 68.1°W	2.82	2008-2016	43,300,000	20
Halley	75.6°S, 26.6°W	4.75	2012-2015	4,300,000	30
SANAE	71.7°S, 2.8°W	4.60	2006-2016	1,780,000	20
Sutherland	32.4°S, 20.6°E	1.78	2007-2011	30,000	0.5
Grahamstown	33.3°S, 26.5°E	1.82	2015-2018	124,000	0.5
Marion Island	46.9°S, 37.9°E	2.68	2009-2016	3,540,000	12
Tihany	46.9°N, 16.9°E	1.83	2007-2017	820,000	4
Gyergyóújfalu	46.7°N, 25.5°E	1.84	2007-2016	120,000	2
Nagycenk/Muck	47.6°N, 17.7°E	1.81	2007-2018	285,000	3
Humain	50.2°N, 5.2°E	2.09	2011-2018	128,000	4
Eskdalemuir	55.3°N, 3.2°W	2.72	2011-2018	10,000	≥ 12
Tvärminne	59.8°N, 23.0°E	3.32	2013-2018	346,000	≥ 15

^{a}At 100 km altitude and at the epoch of 2015 using the IGRF-12 geomagnetic model (Thébault et al., 2015).

3. Results - Regional maps of source lightning and transmission rates

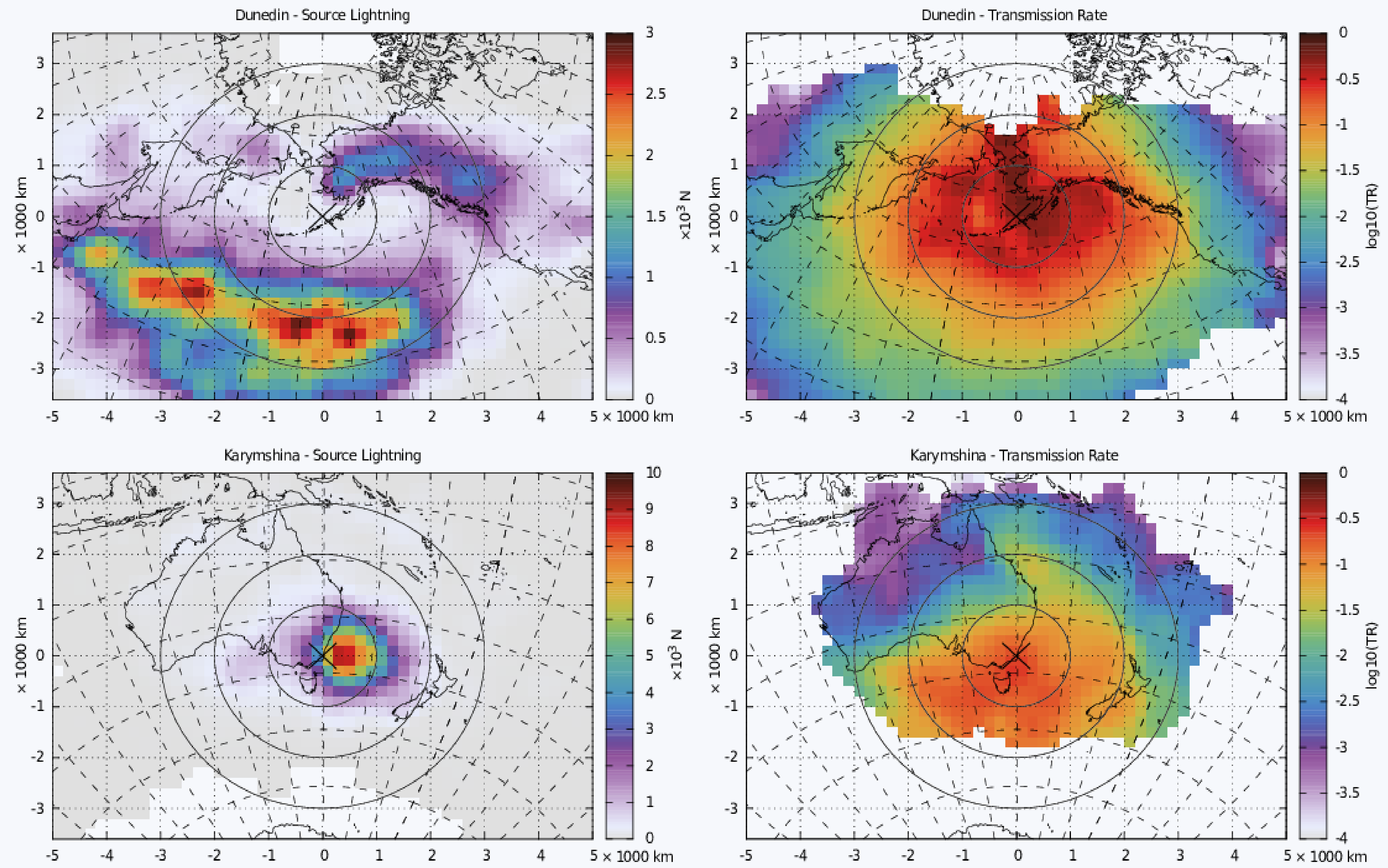

← **Fig. 8.** Regional distribution of source lightning (excess matches) and transmission rate for whistlers detected at Dunedin, New Zealand (top) and Karymshina, Kamchatka (bottom), showing the respective conjugate region). Concentric circles show distances of 1,000, 2,000, and 3,000 km from the conjugate points. Such maps are produced for all 15 stations in this study, see Koronczay (2019).

4. Results - Global map of transmission rates

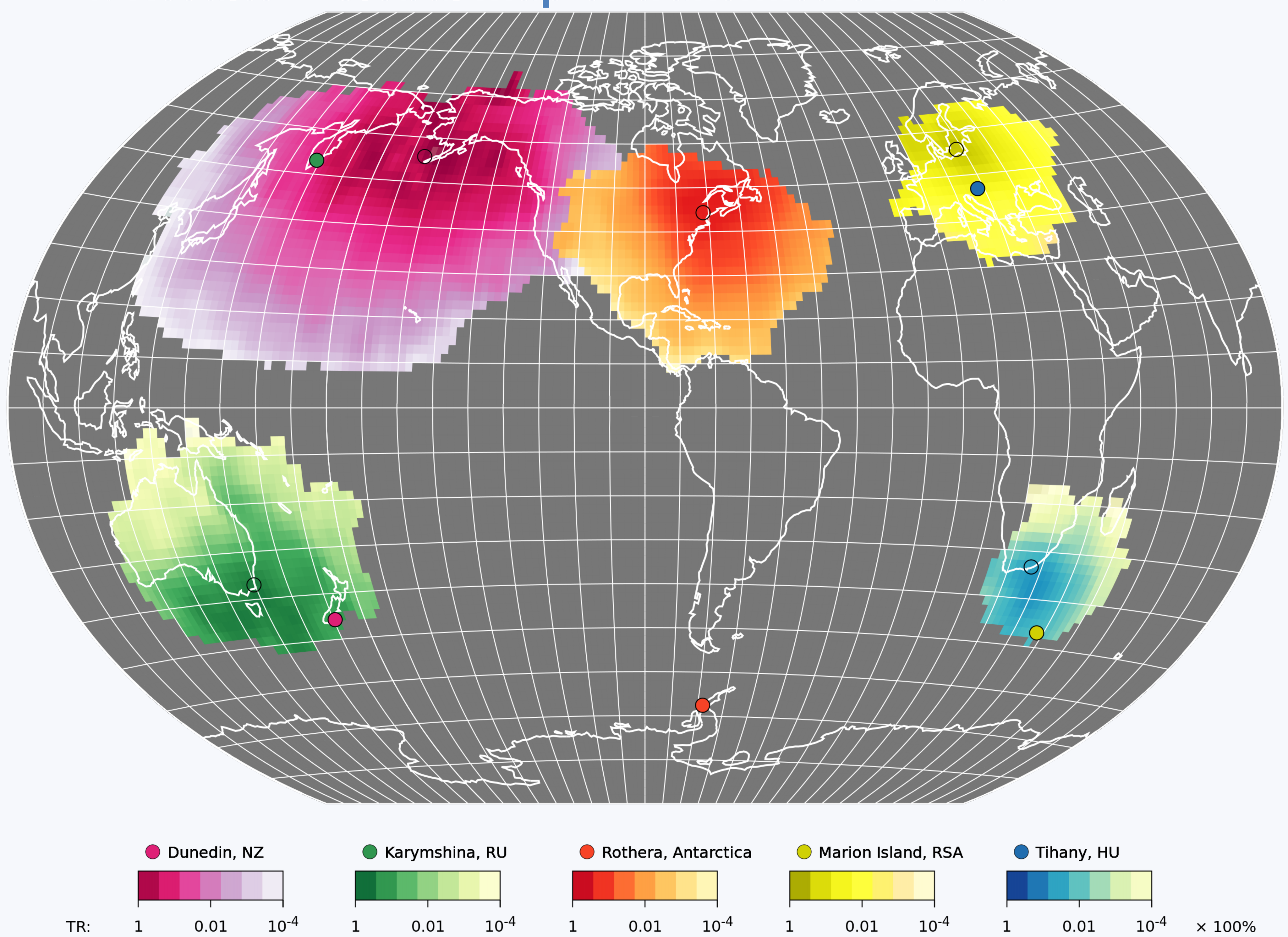

Fig. 9. Distribution of transmission rates on a global map, for five stations in five different geographical regions.

3. Methodology – Distribution of Source Lightning

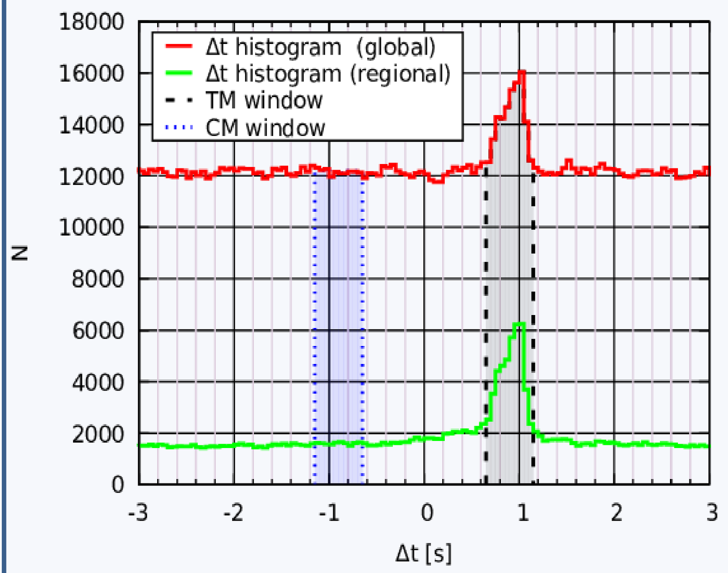

Step 1: Identifying time windows for selection of lightning strokes

← **Fig. 5.** Histogram of time differences between whistlers and lightning strokes, using WWLLN data, global (red) and regional to the conjugate region (green). Δt= t_whistler − t_lightning, and N is the number of lightning-whistler pairs. The peak is due to the tendency of whistlers to occur after causal lightning, the background is caused by chance matches between unrelated whistlers and lightning. Black dashed lines show a time window for the selection of source strokes (TM, total matches). Blue dotted lines show a window of identical length (CM, chance matches) but with whistlers preceding lightning strokes to exclude causality.

Step 2. Determining geographical distribution of source lightning

→ **Fig. 6(a-c).** “Demonstration of the steps of our method. (a) Total matches: distribution of all lightning strokes in the positive time window (lightning preceding whistlers, see Figure 1) Pixel size is 2 ◦ × 2 ◦ ; color represents the number of matched strokes (N) in the given pixel. (b) Chance matches: distribution of lightning activity in the negative time window (lightning following whistlers, excluding causality, representing purely chance matches between the two). (c) Excess matches: difference between total matches and chance matches.

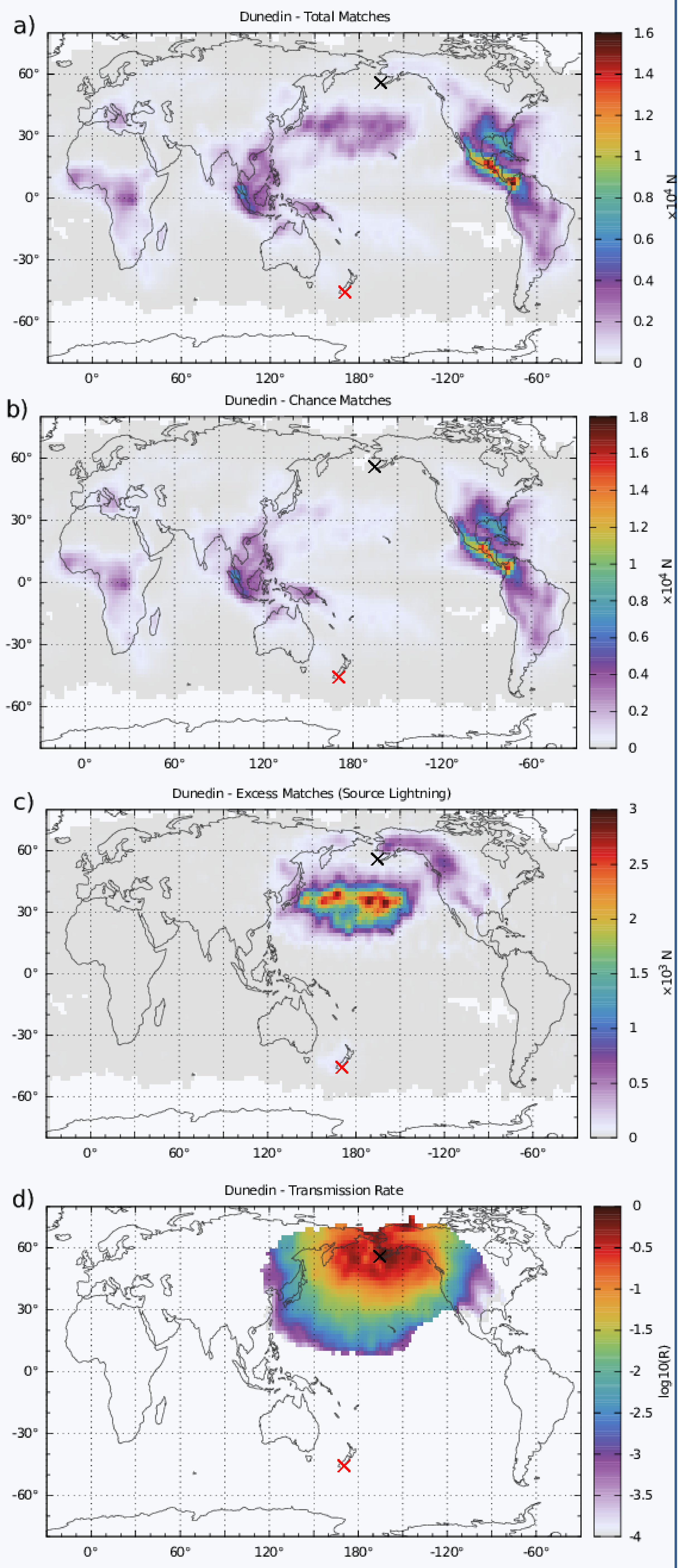

Transmission rates

Step 3. Normalizing the distribution maps with lightning activity

↘ **Fig. 6(d).** Transmission rate (TR) or the number of excess strokes divided by the climatology shown in Figure 3 or the total number of WWLLN lightning strokes over the same time period. Transmission rate (R) is shown only in the area of significant source lightning. All maps are smoothed using a 3 × 3 pixel Gaussian kernel. The red cross marks the location of the whistler recording station; the black cross marks its geomagnetic conjugate point using the IGRF-12 geomagnetic field model.

↓ **Fig. 7.** “Climatology” or total number of WWLLN lightning strokes over the entire measurement period of the whistler station in question (Dunedin, 2007–2017).

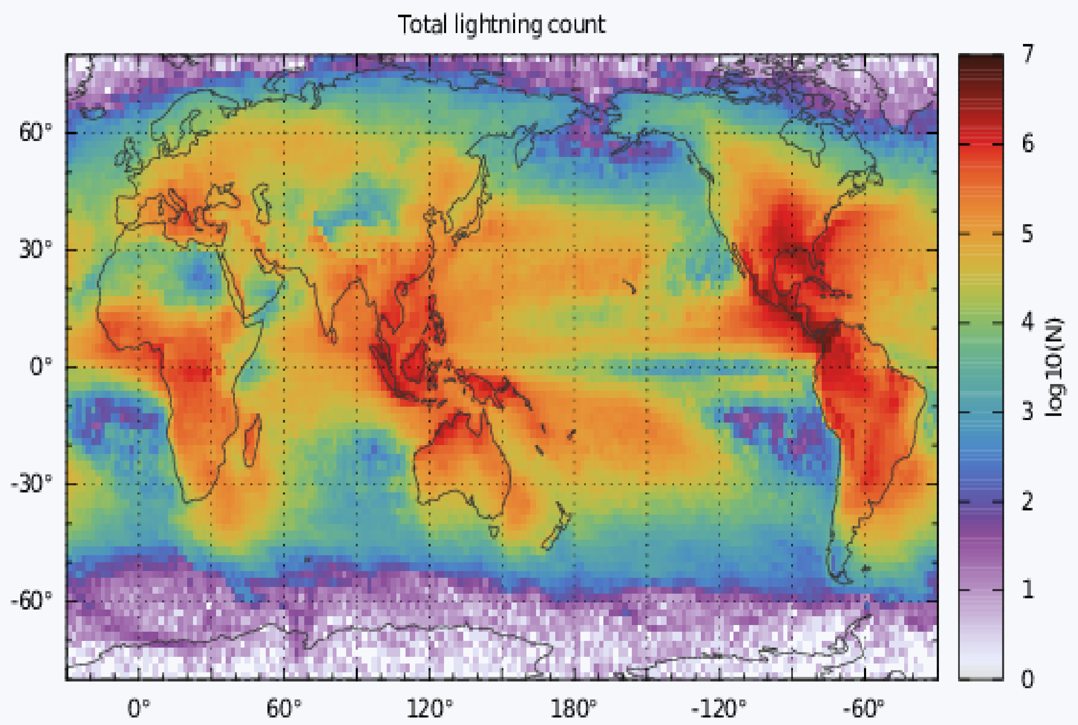

Conclusion

Remarkably, while our algorithm is blind to the location of the detector station (it is not part of the input, it's output, the source strokes shows up around the conjugate point (see Fig. 6c), as expected from theory. Our work supersedes earlier contradicting results (Collier 2010).

- All whistler source regions are centred around the geomagnetic conjugate point of the relevant whistler detector location, and may extend to 2-3 thousand km
- Transmission rates decrease with increasing distance from the conjugate point
- At the moment, transmission rates between stations are not directly comparable (see Fig. 10.)

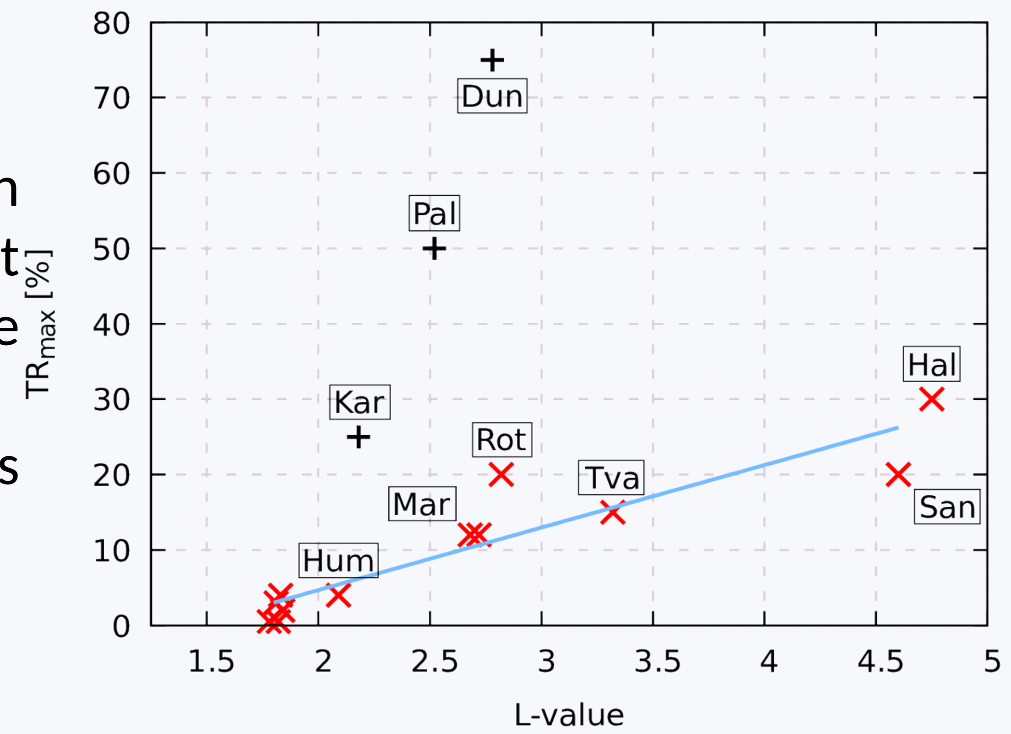

Fig. 10. Maximal transmission rate at each station vs. the L-value of the station. A trend is apparent, with the exception of three points (Karymshina, Dunedin, and Palmer), which we considered outliers (due to extremely good signal quality). Observed transmission rates are sensitive to local electromagnetic noise (and whistler amplitudes).

Outlook

- Having identified the source regions, follow-up study will focus on the temporal changes in the lightning-to-whistler transmission rate, such as: effects of time of day, year, solar cycle, geomagnetic conditions etc.
- In the transmission rate, separation of other effects (lightning and storm parameters, and wave-particle interactions in the radiation belts)
- Finding event pairs of between ground stations and LEO satellites
- → calibration, localization

References

Lichtenberger, J., Ferencz, C., Hamar, D., Steinbach, P., Rodger, C. J., Clilverd, M. A., & Collier, A. B. (2010). Automatic whistler detector and analyzer system – Implementation of the analyzer algorithm. *Journal of Geophysical Research, 115,* A12214.

Collier, A. B., Bremner, S., Lichtenberger, J., Downs, J. R., Rodger, C. J., Steinbach, P., & McDowell, G. (2010). Global lightning distribution and whistlers observed at Dunedin, New Zealand. *Annales Geophysicae, 28,* 499–513.

Lichtenberger, J., P. Szegedi, D. Koronczay, S. Pásztor, L. Juhász, P. Steinbach (2017). ESA PECS Final Report on Validation of the plasmaspheric electron density data by simultaneous analysis of WHISPER and Automatic Whistler Detector and Analyzer Network (AWDANet) data. *ESA contract no. 4000115369. Technical Report.*

Koronczay, D., Lichtenberger, J., Clilverd, M. A., Rodger, C. J., Lotz, S. I., Sannikov, D. V., Cherneva, N. V., Raita, T., Darrouzet, F., Ranvier, S., Moore, C. R. (2019). **The Source Regions of Whistlers.** *Journal of Geophysical Research, Space Physics, 124,* 5082-5096.

Acknowledgement

This work was supported by funding from the National Research, Development and Innovation Office of Hungary under grant agreements NN116408 and NN116446. We acknowledge NIIF for awarding us access to supercomputing resources based in Hungary at Debrecen. F. Darrouzet and S. Ranvier acknowledge BIRA-IASB (Royal Belgian Institute for Space Aeronomy), STCE (Solar-Terrestrial Center of Excellence), and BELSPO (Belgian Federal Science Policy Office) for their support.

Download this poster at https://tinyurl.com/DK-ESWW16

or read our open access paper Koronczay et al. 2019, JGR (see References)